Biochemical Engineering Journal 55 (2011) 185–192

Contents lists available at ScienceDirect

Biochemical Engineering Journal

journal homepage: www.elsevier.com/locate/bej

Electrochemical DNA sensor for simultaneous detection of genes encoding two functional enzymes involved in lignin degradation

Zhen Li[a,b], Guangming Zeng[a,b,*], Lin Tang[a,b], Yi Zhang[a,b], Yuanping Li[a,b], Ya Pang[a,b], Jie Luo[a,b], Yuanyuan Liu[a,b]

[a] College of Environmental Science and Engineering, Hunan University, Changsha 410082, PR China
[b] Key Laboratory of Environmental Biology and Pollution Control (Hunan University), Ministry of Education, Changsha 410082, PR China

ARTICLE INFO

Article history:
Received 10 December 2010
Received in revised form 3 April 2011
Accepted 6 April 2011
Available online 13 April 2011

Keywords:
DNA biosensor
Simultaneous detection
Encoding gene
Functional enzyme
Lignin degradation
Polymerase chain reaction

ABSTRACT

An electrochemical DNA sensor for simultaneous detection of functional genes encoding manganese peroxidase (MnP) and cellobiose dehydrogenase (CDH) on a gold electrode was developed. After two thiolated capture probes assembled on the electrode surface, the electrode was exposed to a monolayer of 6-mercapto-1-hexanol (MCH) solution to prevent nonspecific adsorption of target DNA and detection probes. Horseradish peroxidase–streptavidin (HRP–SA) conjugate and laccase–streptavidin (LAC–SA) conjugate were applied for enzyme-amplified amperometric measurement. The two target genes were simultaneously quantified in the same system. The DNA conformation and surface coverage on electrode were characterized by impedance spectroscopy and cyclic voltammetry. The amperometric current responses to HRP and LAC-catalyzed reactions were linearly related to the common logarithm of two target nucleic acids concentrations, ranging from 1×10^{-11} M to 4×10^{-8} M and 1×10^{-10} M to 4×10^{-8} M. The correlation coefficients were 0.9884 and 0.9881, and the detection limits were 6.2×10^{-12} M and 3.0×10^{-11} M, respectively. The effectiveness of this DNA sensor was confirmed by simultaneous detection of two gene fragments extracted from *Phanerochaete chrysosporium* using polymerase chain reaction (PCR) and restriction endonuclease digestion. The DNA biosensor exhibited good selectivity, precision, stability and reproducibility.

1. Introduction

Biodegradation resistance of wood and other lignified materials is directly related to the presence of lignin [1,2]. Lignin is the most abundant natural aromatic polymers in nature and is extremely recalcitrant in an obligate aerobic oxidative process, carried out appreciably only by the white-rot fungi during secondary metabolism [3,4]. The white-rot basidiomycete *Phanerochaete chrysosporium* has become the model system for studying the physiology and genetics of lignin degradation [5]. Manganese peroxidase (MnP) and cellobiose dehydrogenase (CDH), the two key enzymes produced by *P. chrysosporium*, may mutually effect in an extracellular pathway in fungal lignin mineralization [6]. MnP is an extracellular heme-containing enzyme which can oxidize phenolic lignin model compounds and non-phenolic aromatics via radical intermediates [7,8]. Production and optimization of MnP were investigated by employing different agro-industrial wastes and using response surface methodology [9,10]. CDH is an extracellular hemoflavoprotein which has been proposed to prevent the polymerization reactions and increase the rate of depolymerization in depolymerizing lignocellulose [11,12]. Amperometric detection with mediated electron transfer and high pressure liquid chromatography (HPLC) were used to reveal the kinetic model and effect of CDH on lignin model compounds [13,14]. Over the past decade, MnP and CDH encoding genes have been cloned and characterized from a large number of basidiomycete fungi using polymerase chain reaction and molecular screening assays [15–20].

Recently, electrochemical DNA biosensors have received particular attention due to their fast response, high sensitivity and low cost in environmental and microbial analysis [21–25]. The combination of PCR amplification and DNA sensor was also utilized to improve the detection sensitivity [26,27]. Our group has developed an electrochemical DNA sensor based on the sandwich hybridization recognition of target sequence of lignin peroxidase genes [28], and the simultaneous determination of lignin peroxidase and manganese peroxidase activities using artificial neural networks was also studied [29]. Several papers have proposed that CDH displayed a synergism with MnP during lignin biodegradation and also discussed the relationship between the two enzymes [30,31]. In order to understand the synergistic effects of CDH and

* Corresponding author at: College of Environmental Science and Engineering, Hunan University, Changsha 410082, PR China. Tel.: +86 731 88822754; fax: +86 731 88823701.
E-mail addresses: happylizhen@yeah.net (Z. Li), zgming@hnu.cn (G. Zeng).

1369-703X/$ – see front matter © 2011 Elsevier B.V. All rights reserved.
doi:10.1016/j.bej.2011.04.006

Table 1
Sequences of oligonucleotides used in biosensor.

Oligonucleotide	Sequence (5′–3′)
Capture probe of MnP (M_1)	HS-$(CH_2)_6$-CTGATGGTGTCGTGTTTCT
Detection probe of MnP (M_2)	GATGCCGTTGTTGGCGGAGAA-biotin
Target oligonucleotide of MnP (M_3)	TTCTCCGCCAACAACGGCATCTTTTTTTTTTTTTTTTTTTTTTTTTTTTTTTTTTTTAGAAACACGACACCATCAG
Two-base-mismatched oligonucleotide of MnP (M_4)	TTCTCCTCCAACAACGGCATCTTTTTTTTTTTTTTTTTTTTTTTTTTTTTTTTTTTTAGAAACACCACACCATCAG
Capture probe of CDH (C_1)	HS-$(CH_2)_6$-TGTCAAAGTGGCAGTTCCCGT
Detection probe of CDH (C_2)	CAGCGAGTGGAGGAAACAA-biotin
Target oligonucleotide of CDH (C_3)	TTGTTTCCTCCACTCGCTGTTTTTTTTTTTTTTTTTTTTTTTTTTTTTTTTACGGGAACTGCCACTTTGACA
Two-base-mismatched oligonucleotide of CDH (C_4)	TTGTTTCCTCCACTCACTGTTTTTTTTTTTTTTTTTTTTTTTTTTTTTTTTACGGGAACTGCCACTTTGATA
Sense primer of MnP (M_5)	CATCCGTCTGACCTTCC
Anti-sense primer of MnP (M_6)	AGCCTGTGCCCTTGAGC
Sense primer of CDH (C_5)	ATTGTTTCCTCCACTCG
Anti-sense primer of CDH (C_6)	CCGCCATTGTTCCACTC

MnP on the recalcitrant aromatic compounds degradation better, establishing an effective and sensitive determination protocol for simultaneously monitoring genes encoding the two enzymes from ligninolytic fungi would be of considerable value [32,33].

In this work, an electrochemical DNA biosensor based on two-enzyme labels was developed for simultaneously detecting the hybridization of MnP and CDH gene fragments from *P. chrysosporium*. The consensus oligonucleotide probes and primers were self-designed and synthesized after Clustal alignment of gene sequences in Gene Bank. Two thiolated capture probes and two biotinylated detection probes were hybridized with target sequences respectively on a gold electrode, and the signals were amplified by horseradish peroxidase (HRP) and laccase (LAC), resulting in the low detection limit and good selectivity. The restriction digestion product of MnP genes and PCR product of CDH genes from *P. chrysosporium* were applied to the DNA detection and the results were consistent with the values from electrophoresis and UV spectrometry. The electrochemical DNA biosensor based upon the functional genes of biodegradation enzymes was convinced to hold a potential for further application in the analysis of microbial community functional diversity [34]. This DNA detection technique in the same system should be a platform for simultaneous determination and identification of multiple species of pathogenic microorganisms and functional genes for environmental pollutant biodegradation.

2. Experimental

2.1. Materials

The oligonucleotide primers and target-specific probes were self-designed by Primer Premier 5.0, which were synthesized by Sangon (Shanghai, China). The two capture probes (M_1 and C_1) were modified with $(CH_2)_6$-SH at 5′ end and another two detection probes (M_2 and C_2) were biotinylated at 3′ end to characterize the sensor performance. Target oligonucleotides (M_3 and C_3) were complementary sequences to both capture probes and detection probes. Two-base-mismatched sequences (M_4 and C_4) were applied to test the selectivity of the DNA biosensor. Two pairs of sense primer and anti-sense primer were used in polymerase chain reaction (PCR) amplifications of *P. chrysosporium* MnP and CDH genes. The sequences of oligonucleotides are shown in Table 1. Horseradish peroxidase–streptavidin conjugate (HRP–SA) and dialysis membranes (molecular weight cut off (MWCO) of 14 Da and 25 Da) were purchased from Dingguo Biotechnology Co., Ltd. (Beijing, China). Laccase (EC 1.10.3.2, 23.3 U mg^{-1}) was from Fluka. Streptavidin (SA), tris (hydroxymethyl) aminomethane (Tris) and 6-mercapto-1-hexanol (MCH) were from Sigma–Aldrich. λDNA/HindIII, Marker I, Marker II, restriction endonuclease XbaI, 2× Taq PCR Master Mix, bromophenol blue buffer (6×), TIANquick Midi Purification Kit and TIANgel Midi Purification Kit were provided by Tiangen Biotech Co., Ltd. (Beijing, China). SYBR Green I was from Bio-Vision, Inc. (Xiamen, China). All chemicals used were of analytical grade or better quality, and all solutions were prepared in deionized water of 18 MΩ purified from a Milli-Q purification system. A sodium chloride–sodium citrate buffer (SSC, 0.3 M NaCl and 0.03 M sodium citrate, pH 8.00) was prepared as the hybridization solution. Phosphate buffer saline (PBS, 67 mM KH_2PO_4 and 67 mM Na_2HPO_4), Tris–HCl buffer (0.1 M Tris adjusted to pH 8.00 with 0.1 M HCl) and Tris–EDTA buffer (TE, 10 mM Tris–HCl and 1 mM EDTA, pH 8.00) were used in this work.

2.2. Apparatus

Electrochemical measurements were carried out on CHI660B electrochemistry system (Chenhua Instrument, Shanghai, China) with a three-electrode system consisting of a gold working electrode with a diameter of 2 mm, a saturated calomel electrode (SCE) and a Pt foil electrode, which were used as the reference electrode and auxiliary electrode, respectively. The PCR reaction was carried out in a Bio-Rad MyCycler (Bio-Rad Laboratories, USA) and the Gel electrophoresis analysis was in a DYY-7C electrophoresis system (Liuyi Instrument, Beijing, China). Gel images were captured on a Gel Doc 2000 imaging system (Bio-Rad Laboratories, USA). An Eppendorf BioPhotometer was used to determine the concentration of gel electrophoresis-purified DNA fragment. A UV-2250UV-vis spectrophotometer (Shimadzu, Japan), a CS501-SP thermostat (Huida Instrument, Chongqing, China), a Model 85-2 magnetic stirring apparatus (Lida Instrument, Shanghai, China) and a Branson200S ultrasonic wave washing machine (Xuyang Instrument, Hebei, China) were used in the assay. The solution pH was measured with a model pHSJ-3 digital acidimeter (Shanghai Leici Factory, China). All the work was done at room temperature (25 °C) unless otherwise mentioned.

2.3. Preparation of laccase–streptavidin conjugate

The synthesis of laccase–streptavidin conjugate (LAC–SA) was achieved in a typical procedure. Five milligrams laccase was dissolved in 1 mL of deionized water and 0.2 mL 0.1 M $NaIO_4$ solution was added under stirring, keeping light-resistant for 20 min at room temperature. The mixture solution was dialyzed with 1 mM sodium acetate buffer (pH 4.40) for 12 h at 4 °C and the pH was adjusted to 9.00 with 0.2 M carbonate buffer (pH 9.50). Then 1 mL 0.02 M carbonate buffer (pH 9.00) containing 2.0 mg streptavidin was added and kept stirring gently under light-resistant condition for 2 h at room temperature. Afterwards, the solution was mixed with 0.1 mL 4.0 mg mL^{-1} $NaBH_4$ and continuously reacted for 2 h at 4 °C, and the mixture was dialyzed with 67 mM PBS (pH 7.38) for 12 h at 4 °C. Furthermore, isometric saturated ammonium sulphate solution was added drop by drop under stirring and was centrifugated with 9000 rpm for 15 min after reacting for 2 h at 4 °C. The pre-

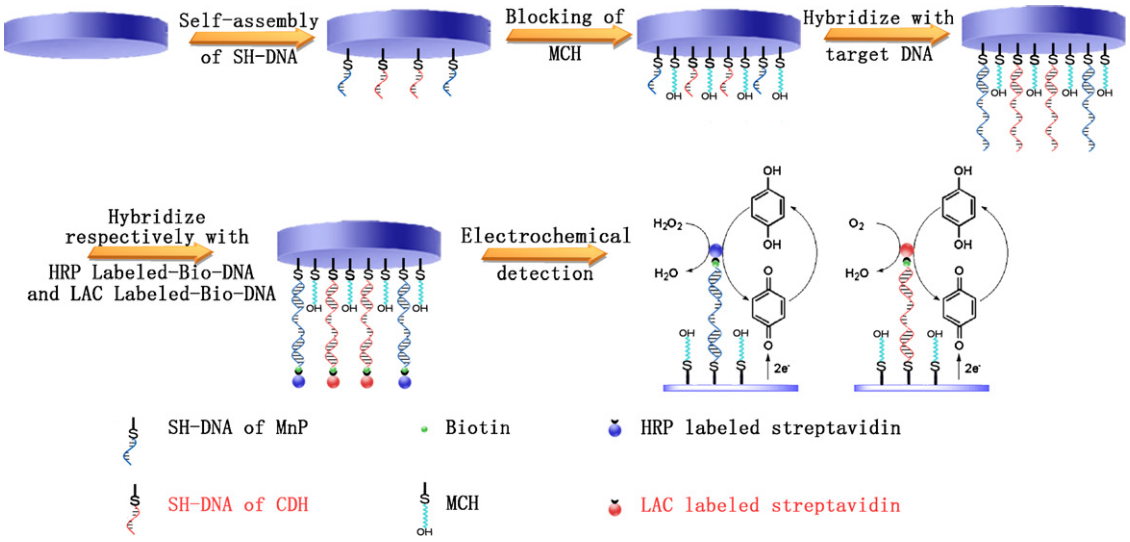

Fig. 1. Schematic diagram of the DNA biosensor fabrication.

cipitate was dissolved in 67 mM PBS (pH 7.38) and dialyzed for 12 h at 4 °C. The supernatant products were collected through centrifugation at 10000 rpm for 30 min and were stored at 4 °C in the refrigerator. The concentration of laccase–streptavidin conjugate was determined by spectrophotometric measurement.

2.4. Preparation of HRP and LAC labeling detection probes

One micromolar per liter biotinylated probe (M_2) was incubated into PBS (pH 6.98) containing HRP–SA with the dilution rate of 1:500 for 30 min at 37 °C. Meanwhile, 1 μM biotinylated probe (C_2) was also incubated into PBS (pH 5.29) containing LAC–SA with the dilution rate of 1:100 for 30 min at 37 °C. Then two of the products were dialyzed respectively with 67 mM PBS (pH 7.38) for 12 h at 4 °C and stored at 4 °C in the refrigerator for use.

2.5. PCR amplification of target DNA from P. chrysosporium

Genomic DNA was extracted from mycelia of *P. chrysosporiumas* using the same method described in our previous work [28]. PCR amplification of MnP and CDH genes were performed to obtain the target fragments for the direct hybridization detection. The 25-μL amplification mixture was consisted of 1 μL of DNA extract, 1 μL 20 nM of each oligonucleotide primers, 12.5 μL 2× Taq PCR Master Mix and 9.5 μL deionized water. The two target genes were both amplified using an initial denaturation at 94 °C for 5 min, and then 30 PCR cycles of three-step amplification. Each of the 30 cycles consisted of 94 °C denaturation for 30 s, 52 °C (MnP) or 48 °C (CDH) anneal for 30 s, and 72 °C extension for 1 min. A final extension was carried out at 72 °C for 5 min, following by a final cooling stage at 4 °C before use. The PCR-amplified products were separated by gel electrophoresis on an agarose gel stained with bromophenol blue and SYBR Green I (Marker II was used for calibration). The target fragments of MnP and CDH were 724 bp and 309 bp, respectively, and were purified using TIANgel Midi Purification Kit.

2.6. Restriction enzyme digestion

Restriction endonuclease digestion was a useful strategy for obtaining sensitive and accurate diagnosis [35,36]. The 724 bp DNA of MnP gene could be cleaved into several short-chain nucleic acids by the restriction endonucleases, therefore the sensitivity and accuracy of the detection could be improved significantly. Eight microliter of the purified fragment was added into 42 μL mixture of deionized water, buffer M and BSA (0.1%) containing 15 U μL^{-1} restriction endonucleases Xba I, followed by incubation at 37 °C for 4 h. The restriction enzyme digestion products were separated by gel electrophoresis with Marker I for calibration, and the target 227 bp fragment was purified using TIANgel Midi Purification Kit.

2.7. Sensor fabrication

The gold electrode surface was polished sequentially with 1, 0.5, 0.05 μm alumina paste, followed by soaking in piranha solution (mixture of 98% H_2SO_4 and 30% H_2O_2 with the volume ratio of 3:1) for 2 h. The ethanol and ultrapure water ultrasonic electrode was scanned by cyclic voltammetry in 0.5 M H_2SO_4 between −0.8 and 1.0 V at 100 mV s^{-1} until a steady state was reached. The mixture solution of 10 μL aliquot of thiolated M_1 and C_1 (20 μM) was dropped onto the electrode surface and kept at 4 °C for self-assembling through thiol-gold bonding. Afterwards, the electrode was copiously rinsed with Tris–HCl buffer and water to remove any nonspecifically adsorbed materials. Two capture probes coated gold electrode was immersed into 400 μL of 1 mM MCH solution for 1 h to improve the quality and stability. Finally, the electrode was washed with Tris–HCl buffer and water to completely substitute the MCH solution for the hybridization reaction [28].

2.8. Hybridization and electrochemical detection

The principle of the biosensor was illustrated in Fig. 1. The thiolated probe immobilized electrode was successively immersed in hybridization solutions (400 μL each) containing two target nucleic acids (M_3 and C_3) at 37 °C for 1 h, followed by thoroughly washing with Tris–HCl buffer and water. Then it was incubated into 400 μL of LAC labeled C_2 solution at 37 °C for 1 h and soaked in 400 μL of HRP labeled M_2 solution at 37 °C for another 1 h. The electrochemical redox current catalyzed by LAC was measured by addition of 5 mM hydroquinone in PBS (pH 5.29) under sustained stirring at a working potential of −0.132 V (vs. SCE). Then the pH was adjusted to 6.98 with NaOH and the current catalyzed by HRP was measured in the same detection system by addition of 1 mM H_2O_2 at a working potential of −0.176 V (vs. SCE). The rapid increase of the reduction current implied that the streptavidin–LAC and streptavidin–HRP have been captured on the electrode. In this

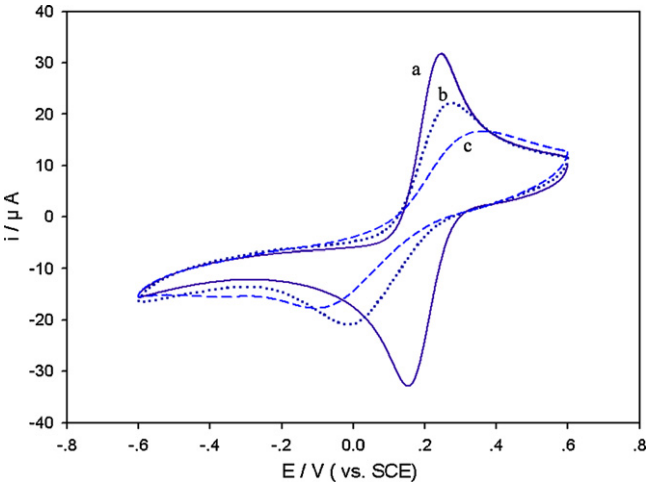

Fig. 2. Cyclic voltammetry diagrams of bare gold electrode (a), gold electrode modified with two capture probes and MCH (b), and the modified gold electrode with two target sequences and detection probes (c), using a 0.1 M KCl solution containing 5.0 mM ferro/ferricyanide, with potential range of −0.6 to 0.6 V, and a scan rate of 100 mV s^{-1} vs. SCE.

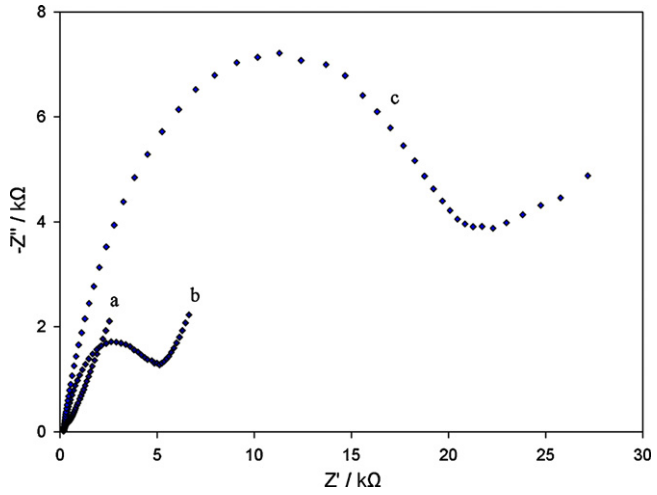

Fig. 3. Electrochemical impedance spectra of bare gold electrode (a), gold electrode modified with two capture probes and MCH (b), and the modified gold electrode with two target sequences and detection probes (c), using a 0.1 M KCl solution containing 5.0 mM ferro/ferricyanide, with frequency range of 0.1–10^5 Hz, a bias potential of 0.19 V vs. SCE and an AC amplitude of 5 mV.

paper, all of the results were the mean value from three parallel measurements.

In order to obtain the target ssDNA, the restriction digestion product of MnP gene and PCR product of CDH gene from *P. chrysosporium* were denatured by heating to 94 °C for 5 min, and were immediately chilled in ice for 30 s [26,37]. The real samples of target genes were applied to the DNA sensor detection as the same procedure used for synthetic oligonucleotides. The concentration of the two target gene fragments were measured by UV spectrometry on Eppendorf BioPhotometer for comparison.

3. Results and discussion

3.1. Electrochemical behaviors of the DNA sensor

We found that hybridizations of thiolated oligonucleotides are dependent on the surface coverage. The precise control over surface coverage was achieved by a two-step method, where the gold substrate was first exposed to the solution of HS-ssDNA, followed by immersing in the solution of 6-mercapto-1-hexanol (MCH). This process could largely remove the nonspecifically adsorbed DNA from the surface. Thus, the majority of surface-bound probes are accessible for specific hybridization with complementary oligonucleotides and are able to discriminate between complementary and non-complementary target oligonucleotides [38].

Electrochemical measurements have long been used to characterize modified electrodes, since they can provide useful information on the interfacial conformations. Fig. 2 shows the cyclic voltammograms obtained for differently modified electrode in 5.0 mM $[Fe(CN)_6]^{3-/4-}$ aqueous solution containing 0.1 M KCl at the scan rate of 100 mV s^{-1} vs. SCE. A pair of well-defined redox peaks of $[Fe(CN)_6]^{3-/4-}$ were shifted significantly (curve b) than that of bare gold electrode (curve a) after the electrode was modified with capture probes and MCH. It was also observed that the redox peak potential difference further increased after hybridization of modified electrode with two target sequences, which evidenced the introduction of complementary DNA increased the negative charge responsible for the repellence of $[Fe(CN)_6]^{3-/4-}$. On the other side, it revealed that the DNA immobilization and hybridization could be effectively operated on current fabricated electrode surface.

Electrochemical impedance spectroscopy of $[Fe(CN)_6]^{3-/4-}$ can also give further information on the impedance changes of the electrode surface during the modification process. The semicircle diameter could represent the electron-transfer resistance, R_{et}, which dominates the electron transfer kinetics of the redox probe at the electrode interface. Meanwhile, the linear part at lower frequencies corresponds to the diffusion process [39]. From the Nyquist plot of the differently modified electrodes shown in Fig. 3, charge transfer resistances of bare gold electrode, capture probes and MCH modified gold electrode, and hybridized gold electrode are about 2.710×10^2, 5.278×10^3, and 2.092×10^4 Ω cm^2, respectively. An almost straight line is observed for the bare gold electrode (curve a), which is typical characteristic of a mass diffusion controlled electron transfer process. After immobilization of two capture probes on the gold electrode and blocking of MCH, the R_{et} was greatly increased (curve b), which could be ascribed to the repellence of probes and resistance of MCH from approaching electrode surface. After hybridization of two ssDNA probes with their complementary sequences, a R_{et} increase of 4 times was obtained than that of the ssDNA and MCH modified electrode (curve c). This attributed to the low conductivity of dsDNA double helix structure, which slowed down the redox reaction of $[Fe(CN)_6]^{3-/4-}$.

3.2. Catalytic reaction mechanisms of biosensor

Laccase is a multicopper phenol oxidase which can directly oxidize hydroquinone by utilizing dioxygen as an oxidant without H_2O_2 as co-substrate [40]. In the reaction, hydroquinone (QH_2) as electron donor for the oxidized form of the enzyme, is mainly converted into quinone and/or free radical product (Q), and then is reduced on the surface of gold electrode at potentials below 0 V (vs. SCE), which efficiently shuttle electrons between laccase redox center and gold electrode surface in a dynamical equilibrium, leading to detectable response current [41]. The reaction equations of the redox process on the electrode surface are described as follows:

$$QH_2 + O_2 \xrightarrow{\text{laccase}} Q + 2H_2O \quad (1)$$

$$Q + 2e + 2H^+ \rightarrow QH_2 \quad (2)$$

Horseradish peroxidase (HRP) is a glycolprotein containing a single protohemin in its active site [42]. It carries out one-electron oxidation on hydroquinone and single two-electron catalysis on H_2O_2 as substrate. The following three steps describe the redox process of hydroquinone catalyzed by HRP. The first step is a

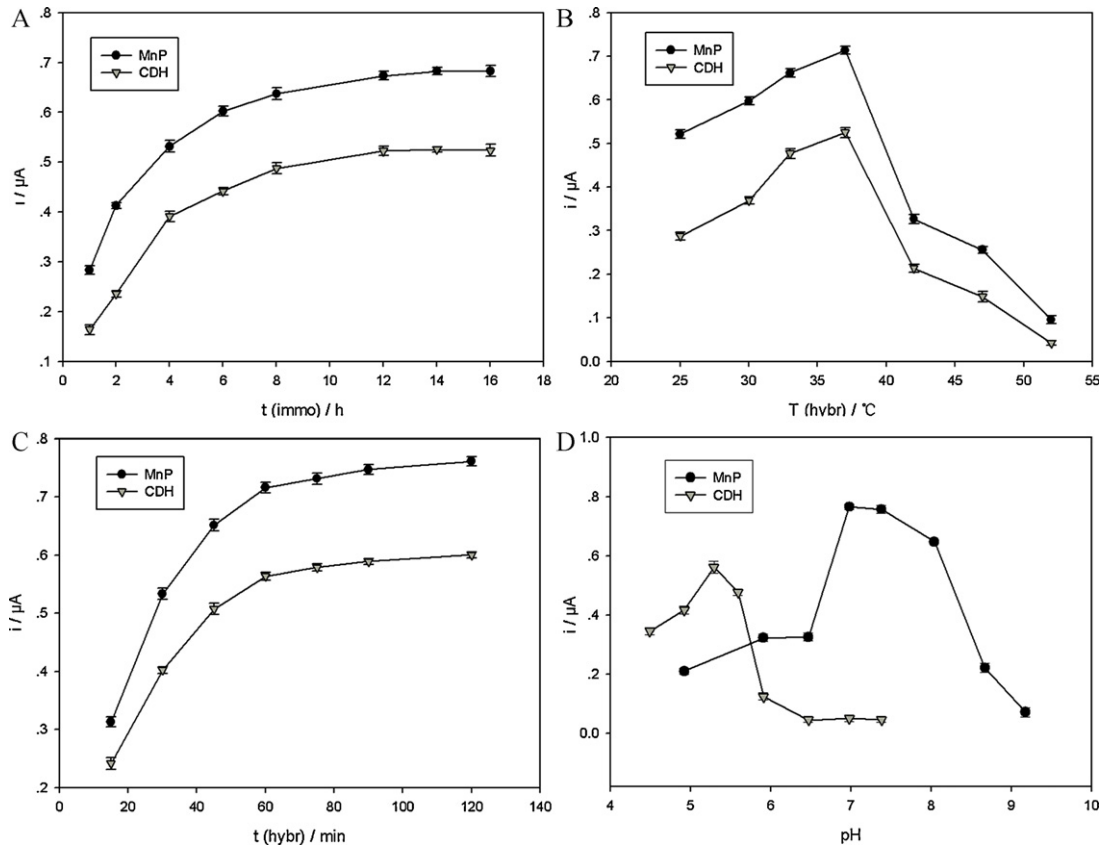

Fig. 4. Optimization of experimental conditions (A) immobilization time with thiolated probes, 20 μM for each probe, (B) hybridization temperature with target sequences, (C) hybridization time with target sequences, (D) pH values of PBS with concentration of 67 mM. The ordinates are all presented as the change of reduction currents by chronoamperometry. The vertical bars designate the standard deviations for the means of three replicative tests.

rapid oxygen atom transfer from hydrogen peroxide to the ferric porphyrin (Fe^{3+}) of HRP to form oxyferryl cation radical haem compound I (HRP I) and water. In the second step, the porphyrin radical cation of HRP I is reduced by the one-electron donor hydroquinone (QH_2) to yield the oxyferryl compound II (HRP II) and the hydroquinone cation radical (Q). In the last step, the enzyme is converted back to its native resting state, HRP (Fe^{3+}), by a subsequent one-electron/two-proton reduction of HRP II by QH_2 to give a second equivalent of Q and water, and Q is reduced on the working electrode to yield detectable electrochemical signals [43]. The reaction equations are described as follows:

$$\text{HRP}\ (Fe^{3+}) + H_2O_2 \rightarrow \text{HRP}\,(I) + H_2O \quad (3)$$

$$\text{HRP}\ \ (I) + QH_2 \rightarrow \text{HRP}\ \ (II) + Q \quad (4)$$

$$\text{HRP}\ \ (II) + QH_2 \rightarrow \text{HRP}\ \ (Fe^{3+}) + Q + H_2O \quad (5)$$

$$Q + 2e + 2H^+ \rightarrow QH_2 \quad (6)$$

3.3. Optimization of experimental conditions

3.3.1. Effect of immobilization time

Two thiolated probes (20 μM) were immobilized on the gold electrode surface by self-assembling in the presence of thiol DNA. The coverage density of the self-assembled probes has a great influence on the sensitivity of sensor. Fig. 4A displays the effect of immobilization time on the change of reduction current responses of two capture probes. It could be observed that the current responses increased fast in the first 6 h and the current continued to enhance with increasing assembly time. After 12 h the steady state was reached, which corresponded to the saturated coverage of the capture probes. Therefore, 12 h of self-assembling time was selected throughout our experiments.

3.3.2. Effects of hybridization temperature and hybridization time

Subsequent studies indicated that the hybridization temperature and hybridization time also acted as very important parameters. The effect of different hybridization temperature is shown in Fig. 4B. It could be seen that the change of reduction current responses increased up to 37 °C and then rapidly declined at high temperature. These reflected that increasing temperature before 37 °C led to higher hybridization efficiency and specificity, and hybridized DNA was unstable and apt to dissociate at higher temperature. Fig. 4C shows the reduction current changes of DNA sensor after hybridization at 37 °C for different hybridization time. The hybridization amounts rose rapidly with time between 15 and 60 min and showed a leveling off after 60 min. Thus, the optimal hybridization temperature was selected as 37 °C and the optimal hybridization time as 60 min.

3.3.3. Effect of pH values of PBS

The pH values of PBS pose the key role during the procedure of electrochemical detection due to the great differences of optimal pH between HRP and LAC. The influence of pH has been determined by comparing the amperometric responses of sensor in different pH range of PBS on the addition of substrates. As demonstrated in Fig. 4D, the change of reduction current responses vary with pH values of PBS and the maximum responses of HRP and laccase were obtained at pH 6.98 and 5.29, respectively, which is similar to that previously reported by Haghighi et al. [44]. For further studies, pH 6.98 and 5.29 of PBS were therefore selected.

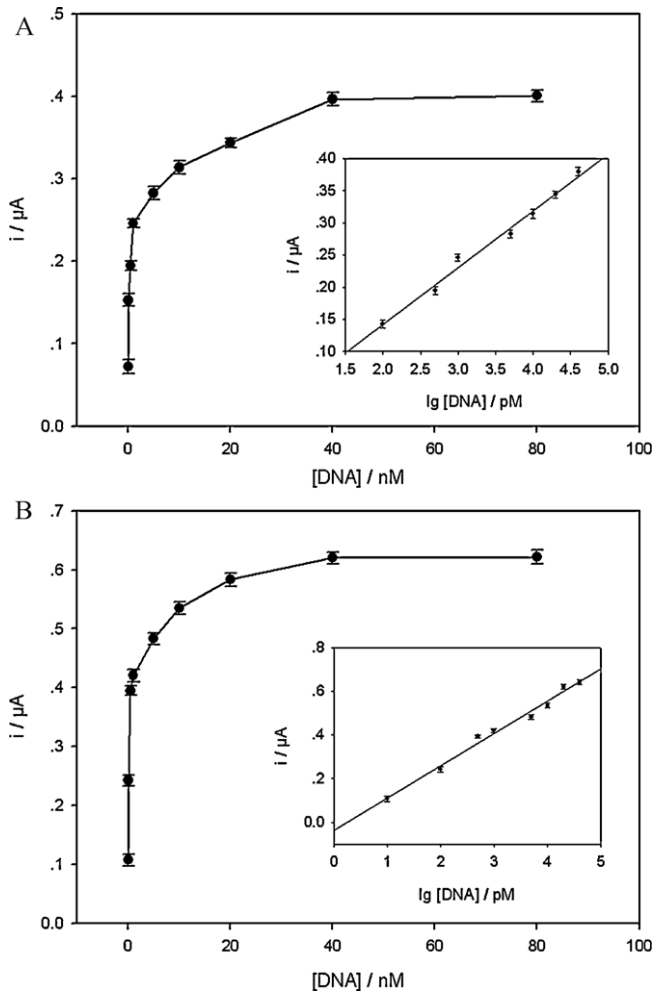

Fig. 5. Relationship between the current response and DNA concentration of (A) CDH DNA and (B) MnP DNA under the optimal experimental conditions. Inset: linear regression of current response vs. the common logarithm of target DNA concentration. The change of reduction currents by chronoamperometry (on ordinate) is presented as a function of the common logarithm of target DNA concentration (on abscissa). The vertical bars designate the standard deviations for the means of three replicative tests.

3.4. Analytical performance for the detection of synthesized oligonucleotides

Under the optimal experimental conditions, Fig. 5A shows the change of reduction currents of the DNA sensor for different concentrations of CDH synthesized target oligonucleotides by chronoamperometry after the addition of hydroquinone to PBS (pH 5.29) under stirring. The current responses increase linearly with the common logarithm of the target nucleic acid concentrations in the range from 1×10^{-10} M to 4×10^{-8} M and the detection limit is 3.0×10^{-11} M (S/N = 3), which resulted in a current signal that equaled the mean value of background signals plus three times standard deviation of background signals. The corresponding regression equation is as follows, and the correlation coefficient is 0.9881:

$$I/\mu A = 0.0886 \times lg(C/pM) - 0.0359 \quad (7)$$

The change of reduction currents of MnP synthesized target DNA were also detected by chronoamperometry in the same system after the addition of H_2O_2, shown in Fig. 5B. With the increase of the DNA concentration, the current change increased rapidly and the steady-state current was reached close to 40 nM. The linear range of MnP target oligonucleotides is 1×10^{-11} M to 4×10^{-8} M and the detection limit is 6.2×10^{-12} M (S/N = 3), which resulted in a current signal that equaled the mean value of background signals plus three times standard deviation of background signals. The corresponding regression equation is as follows, and the correlation coefficient is 0.9884:

$$I/\mu A = 0.0141 \times lg(C/pM) - 0.0230 \quad (8)$$

3.5. Reproducibility and stability of biosensor

The repeatability of the sensor was examined by determination of the same DNA concentration of three consecutive. The average of the relative standard deviations of CDH and MnP genes were 3.5% and 4.3%, which guaranteed the precision of the biosensor. The stability of the immobilized DNA probes on electrode was also investigated. The amperometric responses of two capture probes modified electrode to target DNA retained 86% and 88% of their initial responses after a 15-day storage at 4 °C, which indicated the good stability of the biosensor.

3.6. Selectivity and interference of biosensor

The selectivity of the biosensor was evaluated by analyzing fully complementary and two-base-mismatched sequences under the same optimized hybridization condition and DNA concentration, shown in Fig. 6A and B. The current increment of the complementary sequences of CDH and MnP were 0.42 μA and 0.76 μA, whereas 0.07 μA and 0.13 μA were detected for the two-base-mismatched sequences. The current responses were reduced to 17.3% and 17.2%, respectively, which exhibited good discrimination between complementary and mismatched oligonucleotides.

To evaluate the interference between LAC and HRP presented in the same detection system, the current responses of HRP catalyzed reaction under the natural and nitrogen flow conditions were investigated. The current response catalyzed by HRP was measured in PBS (pH 6.98) containing 5 mM hydroquinone by addition of 1 mM H_2O_2 at a working potential of −0.176 V (vs. SCE) under the natural condition. For comparison, pure nitrogen was bubbled through the PBS (pH 6.98) containing 5 mM hydroquinone during the progress of catalysis to remove the dissolved oxygen as much as possible, because LAC might oxidize hydroquinone by utilizing dioxygen in solution containing H_2O_2. Fig. 7 displays that the current responses of HRP under the two different conditions are approximately the same, which inferred that the catalyzed activity of LAC was strongly inhibited when the pH was up to 6.98. That could also be interpreted in Fig. 4D. Therefore, the changes of current with the addition of H_2O_2 were considered as the responses produced by HRP catalyzed reaction, which quantified the concentration of MnP target genes [45].

3.7. Simultaneous detection of MnP and CDH genes from P. chrysosporium

The denatured ssDNA of MnP and CDH fragments from *P. chrysosporium* genomic DNA was applied to the DNA sensor detection after PCR amplification and restriction-enzyme digestion. The gel electrophoresis photos of extracted genomic DNA, PCR products of MnP and CDH genes, and digested products of MnP genes can be found in Fig. 8. The electrophoresis shown in Fig. 8A confirmed the successful extraction of genomic DNA of 23 kb by the proposed method. The target fragments of MnP gene (724 bp) and CDH gene (309 bp) were amplified with high purity by using the designed primers and appropriate PCR amplication protocol, as demonstrated in Fig. 8B. Digested products were separated by gel electrophoresis, respectively, shown in Fig. 8C, which indicates that

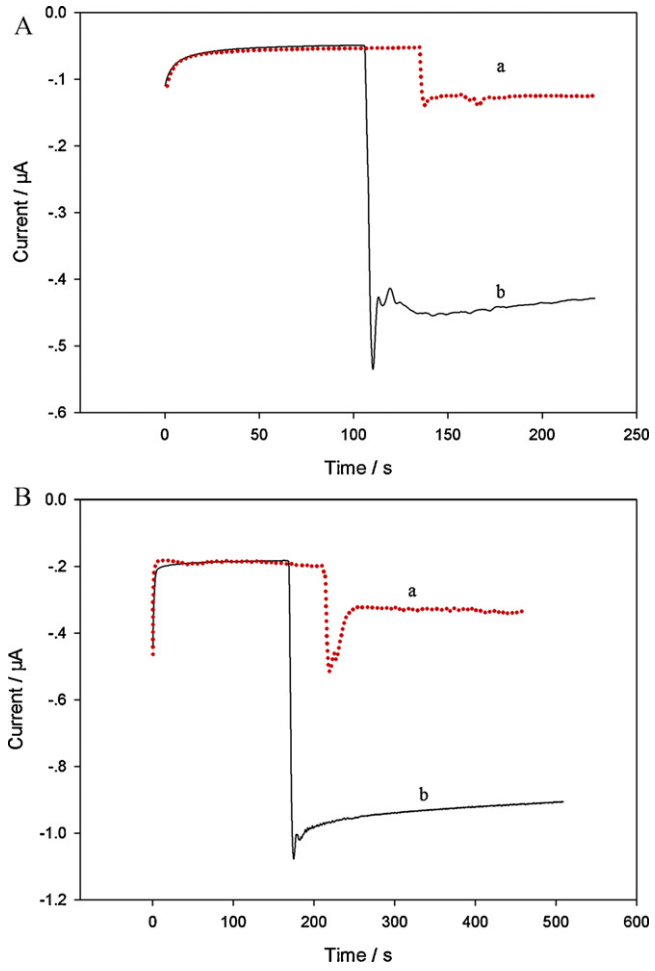

Fig. 6. (A) The current responses of CDH DNA with concentration of 40 nM in 67 mM PBS (pH 5.29) at a working potential of −0.132 V (vs. SCE): (a) two base mismatched ssDNA and (b) complementary ssDNA. (B) The current responses of MnP DNA with concentration of 40 nM in 67 mM PBS (pH 6.98) at a working potential of −0.176 V (vs. SCE): (a) two base mismatched ssDNA and (b) complementary ssDNA.

XbaI could cleave the 724 bp DNA into three short-chain nucleic acids and the fragment of 227 bp was the target for the DNA sensor detection. As the same procedure used for the synthetic oligonucleotides, the 227 bp of MnP gene and 309 bp of CDH gene were captured on the electrode by hybridizing with the complementary capture probes, respectively.

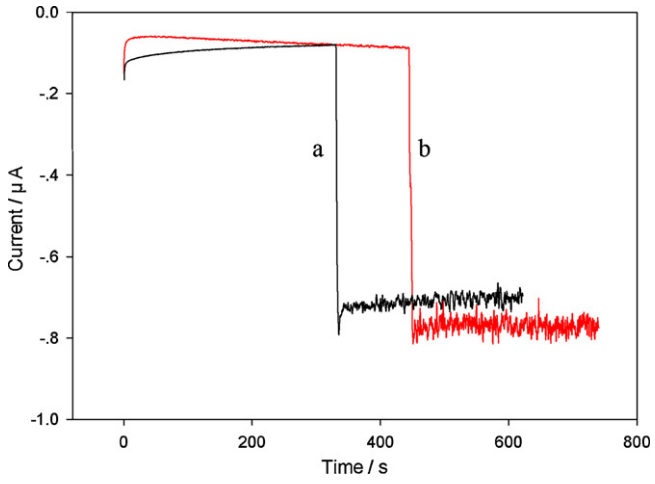

Fig. 7. The current responses of MnP DNA with concentration of 20 nM in 67 mM PBS (pH 6.98) at a working potential of −0.176 V (vs. SCE) (a) under nitrogen flow condition, (b) under the natural condition.

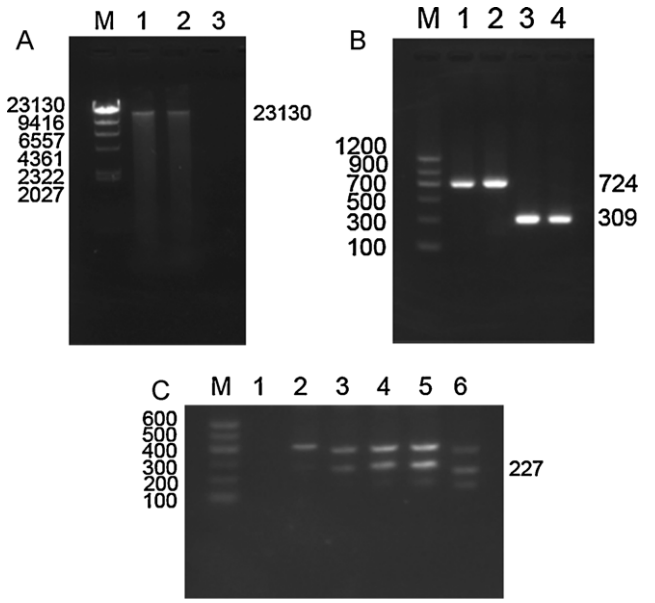

Fig. 8. Gel electrophoresis photos (A) extracted genomic DNA from *P. chrysosporium* (Lanes 1 and 2) using λ DNA/HindIII marker (Lane M) and blank control (Lane 3). (B) PCR products of MnP (Lanes 1 and 2) and CDH (Lanes 3 and 4) genes obtained after amplification with self-designed primers with Marker II (Lane M). (C) Restriction-enzyme digestion products of MnP genes (Lanes 1–6) with Marker I (Lane M). The addition amounts of PCR product in the digestion from left to right are 0 μL, 2 μL, 4 μL, 6 μL, 8 μL and 10 μL.

Table 2
The detection results of MnP and CDH fragment samples from *Phanerochaete chrysosporium* by the DNA sensor and UV spectrometry.

Concentration calibrated by UV spectrometry (nM)		Average concentration recovered by DNA sensor (nM)	Recovery (%)
MnP	0.63	0.54 ± 0.12	85.71
	2.98	2.65 ± 0.27	88.93
	8.41	9.06 ± 0.74	107.73
	17.76	18.93 ± 1.25	106.59
	26.82	25.13 ± 1.82	93.70
CDH	1.17	0.98 ± 0.26	83.76
	6.25	5.44 ± 0.85	87.04
	13.94	15.52 ± 1.69	111.33
	20.65	19.40 ± 1.38	93.95
	29.84	31.97 ± 2.21	107.14

The concentration of the nucleic acids directly corresponded to the electrochemical responses of HRP and LAC labeled on the electrode. The comparison between MnP and CDH fragment samples from *P. chrysosporium* genomic DNA by the DNA sensor and UV spectrometry were shown in Table 2. The detection results from the DNA sensor are in accordance with the reference values deduced from UV spectrometry, with the average recovery ratio of 96.5% and 96.6%, respectively.

4. Conclusion

This study demonstrated the feasibility of simultaneous detection of MnP and CDH genes in the same system by DNA biosensor at low levels. The DNA conformation and surface coverage on electrode were characterized by impedance spectroscopy and cyclic voltammetry. The amperometric current responses were linearly related to the common logarithm of the two target nucleic acids concentrations in the range from 1×10^{-11} M to 4×10^{-8} M and 1×10^{-10} M to 4×10^{-8} M, with the detection

limits of 6.2×10^{-12} M and 3.0×10^{-11} M. The optimized experimental conditions enhanced the sensitivity and stability and the successful discrimination between complementary target DNA and two-base mismatched DNA displayed a good selectivity for the biosensor. The combination of PCR amplification and restriction-enzyme digestion was demonstrated to be a useful strategy for obtaining sensitive and accurate diagnosis in simultaneously detecting two genes from extracted DNA samples of *P. chrysosporium*. The electrochemical detection results of real samples from *P. chrysosporium* genomic DNA were in good agreement with UV spectrometry.

More research into the changes of functional enzymes involved in microbial degradation in combination with advanced bioinformatics approaches is needed to develop the detection technologies from environmental samples. The DNA sensor presented here is a promising step to study the mutual relationship between two functional genes for environmental pollutant biodegradation. Furthermore, this detection technology should be a simple and rapid method of multiple species and trace samples in gene diagnosis.

Acknowledgements

The study was financially supported by the National Natural Science Foundation of China (Nos. 50608029, 50978088, 50808073), Hunan Provincial Innovation Foundation for Postgraduate (CX2009B080), the National Basic Research Program (973 Program) (No. 2005CB724203), Program for Changjiang Scholars and Innovative Research Team in University (IRT0719), and the Hunan Key Scientific Research Project (2009FJ1010).

References

[1] S. Shleev, P. Persson, G. Shumakovich, Y. Mazhugo, A. Yaropolov, T. Ruzgas, L. Gorton, Laccase-based biosensors for monitoring lignin, Enzyme Microb. Technol. 39 (2006) 835–840.
[2] M. Tuomela, M. Vikman, A. Hatakka, M. Itävaara, Biodegradation of lignin in a compost environment: a review, Bioresour. Technol. 72 (2000) 169–183.
[3] T. Johjima, N. Itoh, M. Kabuto, F. Tokimura, T. Nakagawa, H. Wariishi, H. Tanaka, Direct interaction of lignin and lignin peroxidase from *Phanerochaete chrysosporium*, Biochemistry 96 (1999) 1989–1994.
[4] D.K. Arora, R.P. Elander, K.G. Mukerji, Fungal degradation of lignin: biotechnological applications, Fungal Biotechnol. 4 (1992) 763–822.
[5] D. Cullen, Recent advances on the molecular genetics of ligninolytic fungi, J. Biotechnol. 53 (1997) 273–289.
[6] L. Hildén, G. Johansson, G. Pettersson, J.B. Li, P. Ljungquist, G. Henriksson, Do the extracellular enzymes cellobiose dehydrogenase and manganese peroxidase form a pathway in lignin biodegradation, FEBS Lett. 477 (2000) 79–83.
[7] M. Hofrichter, Review: lignin conversion by manganese peroxidase (MnP), Enzyme Microb. Technol. 30 (2002) 454–466.
[8] A.T. Marítnez, Molecular biology and structure–function of lignin-degrading heme peroxidases, Enzyme Microb. Technol. 30 (2002) 425–444.
[9] F. Gassara, S.K. Brar, R.D. Tyagi, M. Verma, R.Y. Surampalli, Screening of agro-industrial wastes to produce ligninolytic enzymes by *Phanerochaete chrysosporium*, Biochem. Eng. J. 49 (2010) 388–394.
[10] L. Levin, C. Herrmann, V.L. Papinutti, Optimization of lignocellulolytic enzyme production by the white-rot fungus *Trametes trogii* in solid-state fermentation using response surface methodology, Biochem. Eng. J. 39 (2008) 207–214.
[11] P. Ander, The cellobiose-oxidizing enzymes CBQ and CBO as related to lignin and cellulose degradation—a review, FEMS Microbiol. Rev. 13 (1994) 297–312.
[12] J. Fang, F. Huang, P.J. Gao, Optimization of cellobiose dehydrogenase production by *Schizophyllum commune* and effect of the enzyme on kraft pulp bleaching by ligninases, Process. Biochem. 34 (1999) 957–961.
[13] G. Henriksson, L.M. Zhang, J.B. Li, Is cellobiose dehydrogenase from *Phanerochaete chrysosporium* a lignin degrading enzyme, Biochim. Biophys. Acta 1480 (2000) 83–91.
[14] L. Stoica, T. Ruzgas, L. Gorton, Electrochemical evidence of self-substrate inhibition as functions regulation for cellobiose dehydrogenase from *Phanerochaete chrysosporium*, Bioelectrochemistry 76 (2009) 42–52.
[15] D.M. Chen, A.F.S. Taylor, R.M. Burke, J.W.G. Cairney, Identification of genes for lignin peroxidases and manganese peroxidases in ectomycorrhizal fungi, New Phytol. 152 (2001) 151–158.
[16] T.J. Dumonceaux, K.A. Bartholomew, T.C. Charles, S.M. Moukha, F.S. Archibald, Cloning and sequencing of a gene encoding cellobiose dehydrogenase from *Trametes versicolor*, Gene 210 (1998) 211–219.
[17] D.M. Li, N. Li, B. Ma, M.B. Mayfield, M.H. Gold, Characterization of genes encoding two manganese peroxidases from the lignin-degrading fungus *Dichomitus squalens*, Biochim. Biophys. Acta 1434 (1999) 356–364.
[18] S. Lobos, L. Larrondo, L. Salas, E. Karahanian, R. Vicuña, Cloning and molecular analysis of a cDNA and the Cs-mnp1 gene encoding a manganese peroxidase isoenzyme from the lignin-degrading basidiomycete *Ceriporiopsis subvermispora*, Gene 206 (1998) 185–193.
[19] S.M. Moukha, T.J. Dumonceaux, E. Record, F.S. Archibald, Cloning and analysis of *Pycnoporus cinnabarinus* cellobiose dehydrogenase, Gene 234 (1999) 23–33.
[20] M. Tello, G. Corsini, L.F. Larrondo, L. Salas, S. Lobos, Characterization of three new manganese peroxidase genes from the ligninolytic basidiomycete *Ceriporiopsis subvermispora*, Biochim. Biophys. Acta 1490 (2000) 137–144.
[21] C.F. Ding, F. Zhao, M.L. Zhang, S.S. Zhang, Hybridization biosensor using 2,9-dimethyl-1,10-phenantroline cobalt as electrochemical indicator for detection of hepatitis B virus DNA, Bioelectrochemistry 72 (2008) 28–33.
[22] X. Mao, J.H. Jiang, X.M. Xu, X. Chu, Y. Luo, G.L. Shen, R.Q. Yu, Enzymatic amplification detection of DNA based on "molecular beacon" biosensors, Biosens. Bioelectron. 23 (2008) 1555–1561.
[23] L. Tang, G.M. Zeng, G.L. Shen, Y.P. Li, Y. Zhang, D.L. Huang, Rapid detection of picloram in agricultural field samples using a disposable immunomembrane-based electrochemical sensor, Environ. Sci. Technol. 42 (2008) 1207–1212.
[24] A. Kaushik, P.R. Solanki, A.A. Ansari, B.D. Malhotra, S. Ahmad, Iron oxide–chitosan hybrid nanobiocomposite based nucleic acid sensor for pyrethroid detection, Biochem. Eng. J. 46 (2009) 132–140.
[25] J. Pan, Voltammetric detection of DNA hybridization using a non-competitive enzyme linked assay, Biochem. Eng. J. 35 (2007) 183–190.
[26] P. Kara, S. Cavdar, A. Berdeli, M. Ozsoz, Electrochemical genoassay design for allele-specific detection of toll-like receptor-2 gene polymorphism, Electroanalysis 19 (2007) 1875–1882.
[27] A. Erdem, D.O. Ariksoysal, H. Karadeniz, P. Kara, A. Sengonul, A.A. Sayiner, M. Ozsoz, Electrochemical genomagnetic assay for the detection of hepatitis B virus DNA in polymerase chain reaction amplicons by using disposable sensor technology, Electrochem. Commun. 7 (2005) 815–820.
[28] L. Tang, G.M. Zeng, G.L. Shen, Y.P. Li, C. Liu, Z. Li, J. Luo, C.Z. Fan, C.P. Yang, Sensitive detection of lip genes by electrochemical DNA sensor and its application in polymerase chain reaction amplicons from *Phanerochaete chrysosporium*, Biosens. Bioelectron. 24 (2009) 1474–1479.
[29] L. Tang, G.M. Zeng, G.L. Shen, Y. Zhang, G.H. Huang, J.B. Li, Simultaneous amperometric determination of lignin peroxidase and manganese peroxidase activities in compost bioremediation using artificial neural networks, Anal. Chim. Acta 579 (2006) 109–116.
[30] M.D. Cameron, S.D. Aust, Cellobiose dehydrogenase–an extracellular fungal flavocytochrome, Enzyme Microb. Technol. 28 (2001) 129–138.
[31] F. Huang, J. Fang, X.M. Lu, P.J. Gao, J.X. Chen, Synergistic effects of cellobiose dehydrogenase and manganese-dependent peroxidases during lignin degradation, Chin. Sci. Bull. 46 (2001) 1956–1961.
[32] T. Johansson, P.O. Nyman, A cluster of genes encoding major isozymes of lignin peroxidase and manganese peroxidase from the white-rot fungus *Trametes versicolor*, Gene 170 (1996) 31–38.
[33] A. Leonowicz, A. Matuszewska, J. Luterek, D. Ziegenhagen, M.W. Wasilewska, N.S. Cho, M. Hofrichter, J. Rogalski, Biodegradation of lignin by white rot fungi, Fungal Genet. Biol. 27 (1999) 175–185.
[34] L. Wu, D.K. Thompson, G. Li, Development and evaluation of functional gene arrays for detection of selected genes in the environment, Appl. Environ. Microbiol. 67 (2001) 5780–5790.
[35] C. Reisinger, A. Kern, K. Fesko, H. Schwab, An efficient plasmid vector for expression cloning of large numbers of PCR fragments in *Escherichia coli*, Appl. Microbiol. Biotechnol. 77 (2007) 241–244.
[36] J.X. Lin, K. Ishikawa, M. Sakamoto, T. Tsunemi, T. Ishiguro, T. Amino, S. Toru, I. Kondo, H. Mizusawa, Direct and accurate measurement of CAG repeat configuration in the ataxin-1 (ATXN-1) gene by "dual-fluorescence labeled PCR-restriction fragment length analysis", J. Hum. Genet. 53 (2008) 287–295.
[37] K. Arora, N. Prabhakar, S. Chand, B.D. Malhotra, *Escherichia coli* genosensor based on polyaniline, Anal. Chem. 79 (2007) 6152–6158.
[38] T.M. Herne, M.J. Tarlov, Characterization of DNA probes immobilized on gold surfaces, J. Am. Chem. Soc. 119 (1997) 8916–8920.
[39] P. Du, H.X. Li, Z.H. Mei, S.F. Liu, Electrochemical DNA biosensor for the detection of DNA hybridization with the amplification of Au nanoparticles and CdS nanoparticles, Bioelectrochemistry 75 (2009) 37–43.
[40] A.I. Yaropolov, O.V. Skorobogat'ko, S.S. Vartanov, S.D. Varfolomeyev, Laccase: properties, catalytic mechanism and applicability, Appl. Biochem. Biotechnol. 49 (1994) 257–280.
[41] L. Tang, G.M. Zeng, J.X. Liu, X.M. Xu, Y. Zhang, G.L. Shen, Y.P. Li, C. Liu, Catechol determination in compost bioremediation using a laccase sensor and artificial neuralnet works, Anal. Bioanal. Chem. 391 (2008) 679–685.
[42] A.M.L. Zatón, E. Ochoa de Aspuru, Horseradish peroxidase inhibition by thiouracils, FEBS Lett. 374 (1995) 192–194.
[43] L. Tang, G.M. Zeng, Y.H. Yang, G.L. Shen, G.H. Huang, C.G. Niu, W. Sun, J.B. Li, Detection. of phenylhydrazine based on lectin-glyco enzyme multilayer-film modified biosensor, Int. J. Environ. Anal. Chem. 85 (2005) 111–125.
[44] B. Haghighi, L. Gorton, T. Ruzgas, L.J. Jönsson, Characterization of graphite electrodes modified with laccase from Trametes versicolor and their use for bioelectrochemical monitoring of phenolic compounds in flow injection analysis, Anal. Chim. Acta 487 (2003) 3–14.
[45] M. Aitichou, R. Henkens, A.M. Sultana, R.G. Ulrich, M.S. Ibrahim, Detection of *Staphylococcus aureus* enterotoxin A and B genes with PCR-EIA and a hand-held electrochemical sensor, Mol. Cell. Probes 18 (2004) 373–377.